J Mater Sci: Mater Electron **(2025) 36:1195**

Energy gap: refractive index in ZnO/Fe/ZnO multilayer prepared by ALD and DC

M. Nabil[1,*], S. S. Fouad[2,*], G. Katona[3], E. Baradács[3,4], and Z. Erdélyi[3]

[1] *Department of Basic Engineering Sciences, Faculty of Engineering (Shoubra), Benha University, Benha, Egypt*
[2] *Department of Physics, Faculty of Education, Ain Shams University, Cairo 11566, Egypt*
[3] *Department of Solid-State Physics, Faculty of Science and Technology, University of Debrecen, P.O. Box400, Debrecen 4002, Hungary*
[4] *Department of Environmental Physics, University of Debrecen, Poroszlay U.6, Debrecen 4026, Hungary*

Received: 5 May 2025
Accepted: 14 June 2025
Published online: 8 July 2025

ABSTRACT

The present work provides a mathematical formulation for the optical energy gap-refractive index relations of Fe layer with different thickness, inserted between two layers of ZnO in the form of ZnO/Fe/ZnO thin film system. The thin films having a multilayer of ZnO/Fe/ZnO have been grown on glass substrates, using atomic layer deposition and DC magnetron sputtering. The crystalline structure of the multilayer thin films was carried out by the X-Ray diffraction while the thickness data and the quality of the layers were checked by using a prepared lamella for each sample using focused ion beam (FIB). The extinction coefficient (k) of the thin film samples was used to calculate the energy band gap (E_g). An explanation for the dependence of Fe interlayer thickness (20, 40, 60 and 80nm) between upper and lower layer of ZnO(80nm) on the optical energy gap and refractive index (n) of the thin film samples and their relationship are presented and discussed using different theories. With increasing the Fe interlayer thickness, the evaluated band gap showed a decrease from 3.77eV to 3.43 eV, while the calculated refractive index was found to increase from 2.20 to 2.27. The optical conductivity, optical dielectric constant, dielectric susceptibility, electronic polarizability, electronegativity, optical basicity and metallization criterion were obtained by several calculations based on the refractive index. By fixing the ZnO thickness and varying the Fe thickness, we can isolate the effects of Fe thickness on the optical properties of ZnO/Fe/ZnO system. The fixed thickness of ZnO enable direct comparison of the optical properties and related parameters across different Fe thickness and hence enabling the design of materials with specific potential applications. Further derivations based on the energy gap – refractive index relations discussed in the context, indicates that the insertion of a metallic layer into oxide layer have high potential that could enhance the quality of remarkable optical properties of ZnO thin film, to be applied for memories applications and allows the performance of the devices, to be optimized.in many industrial and consumer products.

Address correspondence to E-mail: mohammed_diab35@yahoo.com; profsu95@gmail.com

https://doi.org/10.1007/s10854-025-15225-9

1 Introduction

Thin film has attracted worldwide a considerable amount of attraction due to their unique physical, optical, electrical and magnetic properties that leads it to great interest in the area of microelectronics and nanoelectronics among other features [1–3]. Furthermore, they offer remarkable potential applications in various fields.

Zinc oxide is one of the most promising materials for application in nanotechnology and has been invented in the fields of solar cells and especially in the drive device and switching device. ZnO is a strong candidate for the channel layer for the channel layer in thin film transistors (TFTs), because ZnO is transparent to visible wavelength.

As an electronic material, ZnO is extremely important for the control of its inherent defects that control its properties. Recently, many researchers focused on the investigation of the drastically change in structural morphology and optical and electrical properties of ZnO thin film by its addition with transition metal [4, 5] for the memory's applications. The insertion of a metallic layer into an oxide layer allows the performance of any device to be optimized [6–8]. Transparent conductive ZnO films with low resistivity as well as high visible transmittance could be realized by the addition of Cu, Ni and Mn [9–11].

The addition of metal to zinc oxide can improve photo degradation activity. Modification of ZnO by various metals, generally can improve the activity of optical properties, and could be higher compared to pure ZnO.

Relatively little attention has been paid to Fe-doped ZnO thin films [12, 13]. Fe doped ZnO films are synthesis by using several deposition techniques such as sol–gel method, ion -beam sputtering, spray-pyrolysis, magnetron sputtering [3, 14, 15]. Fe is a ferromagnetic material, which can introduce magnetic properties to the ZnO/Mn/ZnO system. The incorporation of Fe into ZnO can modify its optical properties. The Fe as an interlayer can create interesting interface effects between ZnO and Fe. By choosing Fe as an interlayer in ZnO we can explore the potential of ZnO/Fe/ZnO system for various applications including spintronics, optoelectronics and solar cells.

ALD appears as the perfect technique for producing an excellent film of all methods, precise control of the thickness, good crystalline quality by adjusting the ALD cycle ratio of the host and dopant one [16–18]. By utilizing ALD we can create high -quality ZnO -based devices with improved performance, excellent conformity and reliability, we can also control the interface formation between Fe and ZnO, which can impact the device electrical and optical properties. In our previous work in [18] we have determined the tail of the localized state, and we have calculated all the parameters associated with it such as the electron -phonon interaction and the steepness parameter and the skin depth.

In the present work, Fe doped ZnO thin films were deposited onto soda-lime glass substrates using atomic layer deposition and Dc magnetron sputtering as given in details in [18] The main objective of this study is to analyze the impact of Fe thickness in more expansive ways, on the energy gap-refractive index relation and are strongly correlated to several determined parameters by using the refractive index on optical devices that have high potential to be applied on several applications.

2 Experimental procedure

The processing procedures used for preparing the ZnO/Fe/ZnO thin films by increasing the ferrite content were in the same way used in our earlier studies given in [18]. The samples were prepared by a combination of ALD and DC magnetron sputtering. First, 80 nm ZnO was grown on soda-lime glass substrates by ALD (Beneq TFS-200).

Subsequently, Fe layers of different thicknesses (20, 40, 60, 80 nm nominal thickness) were grown on the ZnO layer by magnetron sputtering. Then, 80 nm ZnO layer was deposited again on top of the Fe layers by ALD method. ZnO layers were prepared at 200 °C using water (H_2O) and diethylzinc (DEZ) precursors. The H_2O and DEZ pulses were 300 ms long, while the purge time was 3 s in all cases. In total, 444 cycles were used to grow 80 nm ZnO. Pressure was 6.3×10^{-3} mbar and the sputtering power used was 24 watts. Nevertheless, based on the thermal expansion behaviour of the constituent materials and the deposition sequence, a plausible explanation can be established. The bottom ZnO layer experiences compressive strain after cooling due to the higher contraction of the substrates. The Fe layer deposited at room temperature grows initially strain- free. Upon cooling the Fe contracts more than the ZnO resulting in compressive stress in the upper ZnO layer [16].

The schematic diagram that shows the steps of the preparation of ZnO/Fe/ZnO with different thickness of Fe is illustrated in Fig. 1.

The phase and structure of $ZF_{20}Z$, $ZF_{40}Z$, $ZF_{60}Z$ and $ZF_{80}Z$ were identified using grazing incident X-ray diffraction (GIXRD, Rigaku Smart Lab). The morphology and cross-section images of the four thin films, were performed to confirm the thickness by using FIB to prepare a lamella from each sample. Energy – dispersive X-ray (EDX) analysis is applied along with SEM to analyze the types and the quantity of elements at the surface.

The transmittance and reflectance spectra for the Z F_{20} Z, $ZF_{40}Z$, $ZF_{60}Z$ and $ZF_{80}Z$ thin film samples were determined using UV–Visible spectrophotometer (Shimadzu Model UV-3101 PC) in the spectral range 190 nm—820 nm. Experimentally, the absorption coefficient α was determined from the absorbance by using this simple relation $\alpha = 2.303$ A/t, where A is the absorbance and t are the thickness of thin film. All sample measurements were performed at room temperature. The main factor in this work, the extinction coefficient (K), was obtained by using Murmann' exact equation [19, 20].

3 Results and discussion

3.1 Structural characterization

From the GIXRD results we can conclude the following, as indicated in Fig. 2. The structure of the ZnO corresponds to the hexagonal variant. Based on the intensity ratio of ZnO (002)/ZnO (100), ZnO (002)/ZnO (101) and ZnO (002)/ZnO (110) reflections, the texture of the ZnO layers is different for the 20, 40nm and 60, 80 nm sample pairs, since the ratio changes with a factor of 2–3.

From these measurements it cannot be decided whether both layers are affected or only top layer. Comparing the ZnO (100) and ZnO (101) reflections there is a much smaller change (20%) and this is the case with other reflections too. The results show that ZnO (002) reflection became more intense in case

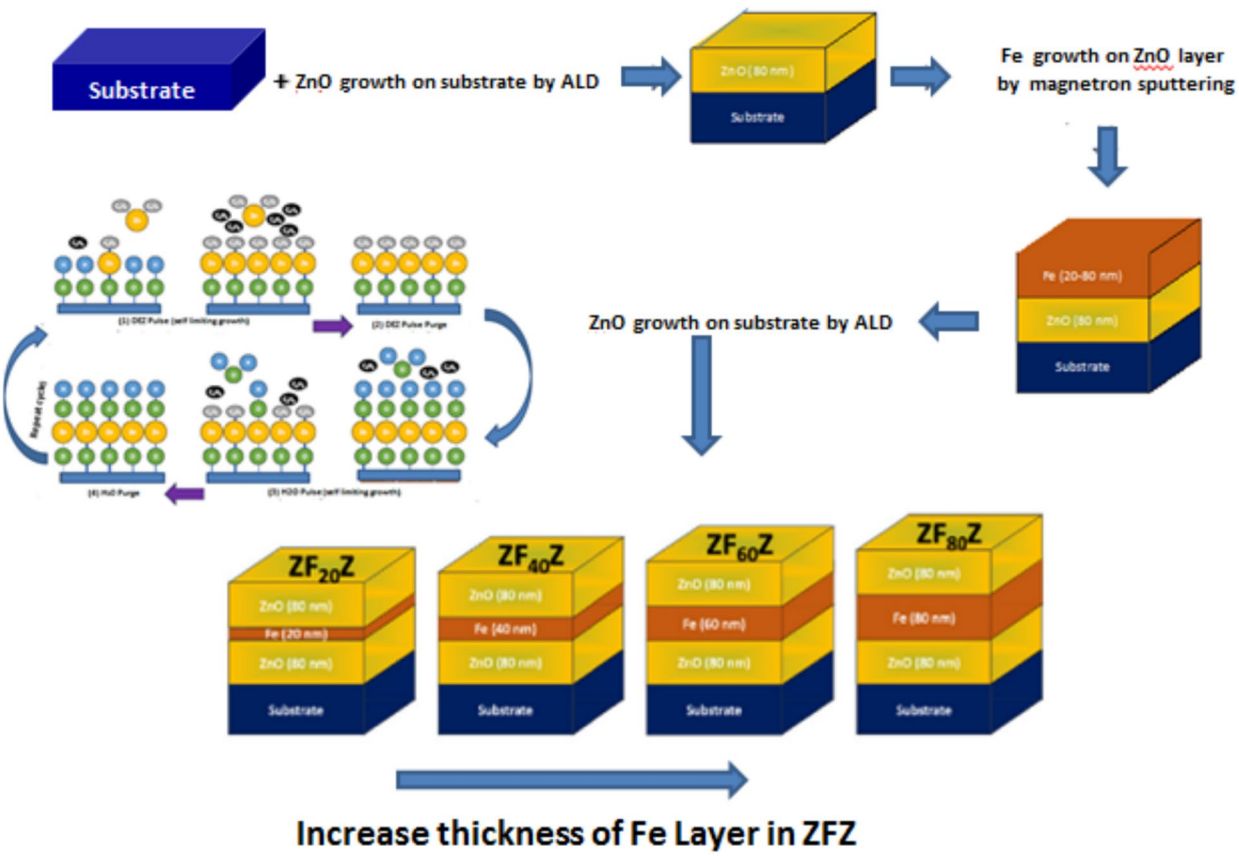

Fig. 1 Schematic cyclic process of the preparation of ZnO/Fe/ZnO by DC magnetron sputtering and ALD

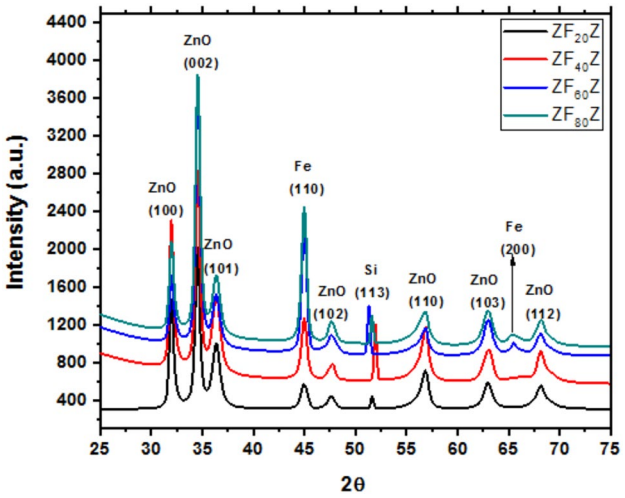

Fig. 2 GIXRD diffraction pattern for $ZF_{20}Z$, $ZF_{40}Z$, $ZF_{60}Z$ and $ZF_{80}Z$ thin films

of thicker Fe layers as compared to the others. The width of the ZnO reflections provides different crystallite sizes from the ZnO (100) and ZnO (002) reflections. In this case the crystallite size is 170-200nm, while from other reflections 8–12 nm is obtained. This suggests elongated crystallites. The Fe layer is probably textured, since for thinner (20, 40 nm) layers only the Fe (110) reflection was detected, while in case of thicker layers the Fe (200) reflection becomes visible, however its intensity is much lower as it can be expected for a non-textured layer. Although GIXRD was performed, our configuration did not allow for the evaluation of in-plan lattice parameters, and hence we could not directly resolve in-plan strain, unlike in [17, 21]. The results from (SEM) of ZnO/Fe/ZnO thin films embedded with the incorporation of different amount of Fe interlayer thickness are depicted in Fig. 3a–d. Using EDX analyses quantitative determination of the concentration of the four samples of the ZnO/Fe/ZnO system was performed by ZAF correction procedure. Figure 3a1–d1, give the results of EDX analysis, which provides the information about the elements present of the particles with an accuracy of 0.5wt%. Concentration below this value indicates the element's clear presence, but the relative error of the measured quantity is significant and should be considered accordingly.

The thickness data and the quality of the layers were checked by a lamella that was prepared from each sample by using FIB as shown in Fig. 4. The thickness data for Fe in four samples $ZF_{20}Z$, $ZF_{40}Z$, $ZF_{60}Z$ and $ZF_{80}Z$ were 20nm, 40nm, 60nm and 80 nm respectively and are in excellent agreement with what we wanted to produce. The cross section of the investigated samples presents a uniform structure without any visible delamination or defects.

3.2 Energy band gap (E_g)

The extinction coefficient (k) is a measure of the fraction of light lost due to the scattering and absorption per unit distance of the participating medium. The absorption coefficient (α) can be calculated from k by using the following relation:

$$\alpha = 4\pi k/\lambda \tag{1}$$

where k is the extinction coefficient, which has been experimentally defined from the transmittance and reflectance curves given before in [18].

The spectral distribution of the extinction coefficient and the absorption coefficient (α) for the four thin film samples of the ZnO/Fe/ZnO thin film samples are shown in Fig. 5a, b respectively. In the high absorption region from which the optical energy band gap E_g is determined, the absorption is characterized by Tauc's relation [22]

$$\alpha h\upsilon = B(h\upsilon - E_g)^r \tag{2}$$

where B is a constant and r is the power factor, with $r = 0.5$ for direct allowed transition. An illustration of the linear fitting of Tauc's plots between $(\alpha h\upsilon)^2$ and the photon energy $h\upsilon$ is depicted in Fig. 5c for different multilayers thin films of the ZnO/Fe/ZnO thin films. The optical band gap values were obtained by extrapolating the linear part of the curves at $(\alpha h\upsilon)^2 = 0$. The comparison values of E_g for the direct allowed transition of $ZF_{20}Z$, $ZF_{40}Z$, $ZF_{60}Z$ and $ZF_{80}Z$ are seen in Fig. 5d. The values of E_g were found to be decreased with the increase of Fe interlayer thickness from 3.77 eV to 3.43eV, as observed in Table 2 As a result of increasing Fe thickness, the magnitude of the thermal mismatch increasing, resulting in stronger compressive strain in the adjacent ZnO, this increase causes a progressive reduction in Eg, as observed in Fig. 5d,due to distortion of the Zn–O bonds and the associated changes in the electronic band structure. The continuous decrease in E_g suggests the potential application of ZnO/Fe/ZnO thin films in photocatalysis and novel energy devices. In order to emphasize the type of electronic transition that has occurred in the four thin

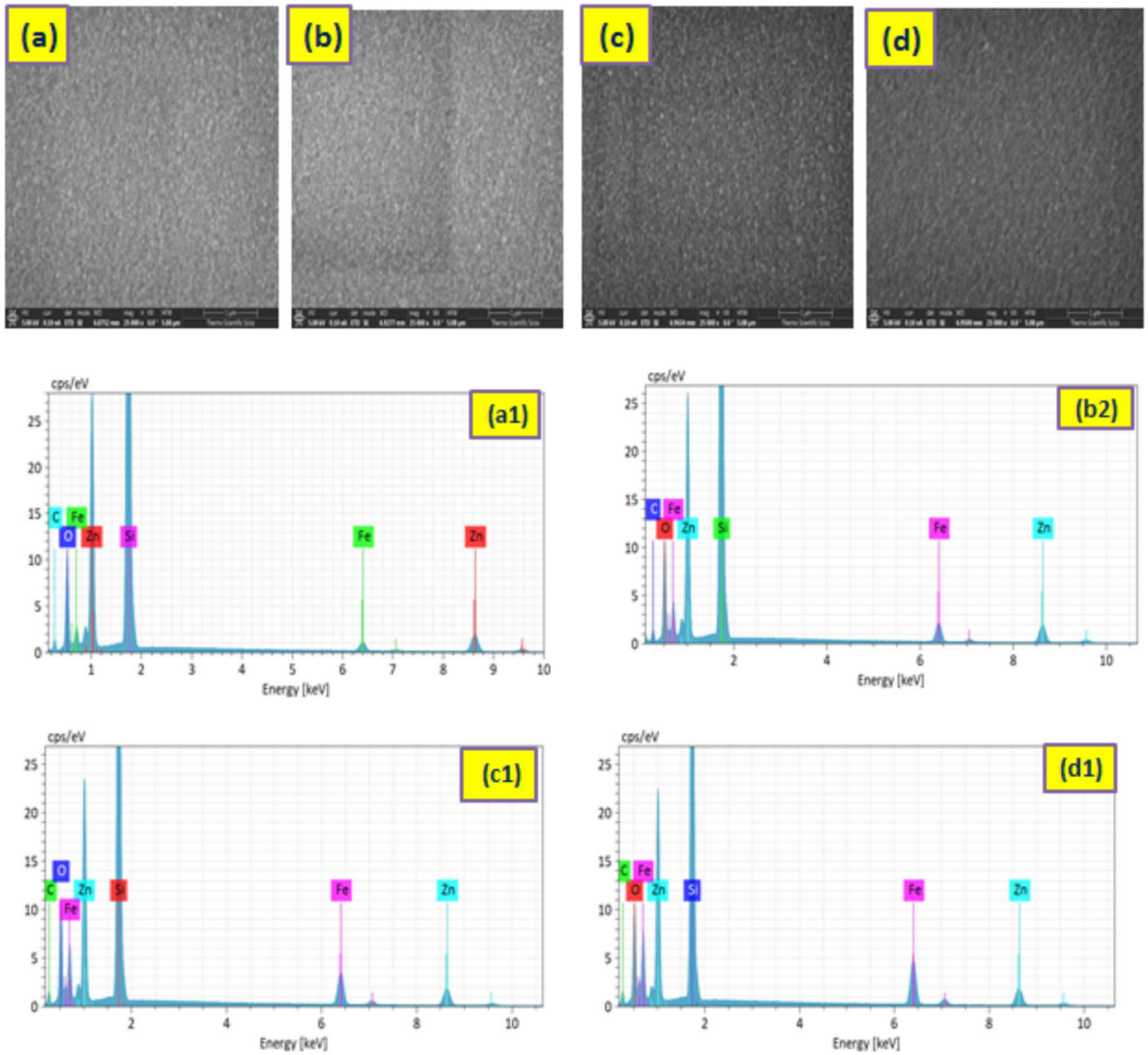

Fig. 3 SEM, EDX for $ZF_{20}Z$, $ZF_{40}Z$, $ZF_{60}Z$ and $ZF_{80}Z$ thin film respectively

films if they were direct or indirect transition, the optical energy gap must first be determined, and then the power factor r can be obtained by using the formula used by [23].

$$ln(\alpha h\nu) = ln(B) + rln\left(h\nu - E_g\right) \tag{3}$$

where B is a constant. By plotting ln $(h\nu - E_g)$ on the x axis, and ln $(\alpha h\nu)$ on the y axis as can be seen in Fig. 6, we obtain a straight line for each of the four thin films understudy, the slope of which determine the power factor r.

The calculated values of the transition power factor for $ZF_{20}Z$, $ZF_{40}Z$, $ZF_{60}Z$ and $ZF_{80}Z$ are approximately equal $\cong 0.5$, as tabulated in Table 1. This process confirms the existence of the direct power transition factor that has been determined earlier via Eq. 2. The above findings agree and in harmony with the results given in [18, 23].

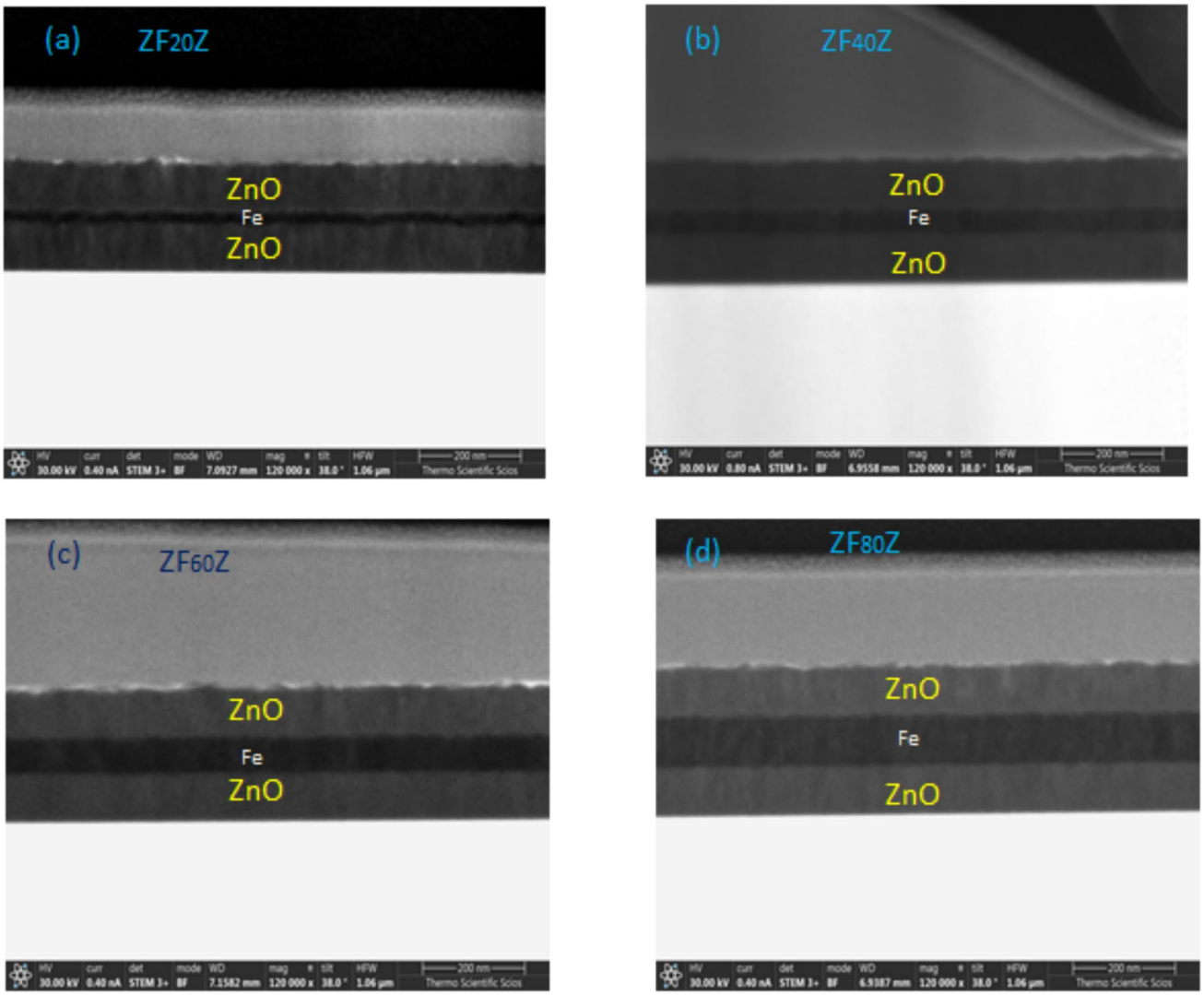

Fig. 4 Cross-section electron micrograph for $ZF_{20}Z$, $ZF_{40}Z$, $ZF_{60}Z$ and $ZF_{80}Z$ thin films respectivlely

3.3 Index of refraction (*n*)

Refractive index is one of the most important fundamental properties of materials and it is related to the local field inside the materials. In optics the refractive index determines how much the path of light is bent or refracted, when entering any material. In order to choose the appropriate materials for optoelectronic application, it is necessary to determine the optical constants such as the refractive index. The evaluation of the refractive index is fundamental parameter for the design of the devices. The higher the number of (n), the slower light travels through the medium, the more the light is bent, this bending by refraction makes it possible to have magnifying glasses or thin films. A group of researchers [9] have attempted to obtain the relationship between the refractive index (n) and optical energy gap E_g but they failed to give realistic explanation, except Moss and Ravindra et al. [9, 24–26]. Therefore, the following equations were found to describe the best fit for obtaining the (n) [9, 24–26].

$$n^4 E_g = 95eV \tag{4}$$

$$n = K\left[E_g\right]^c \tag{5}$$

The values of the constants used in Eq. (5) are, $K = 3.3668$, $C = -0.32234$

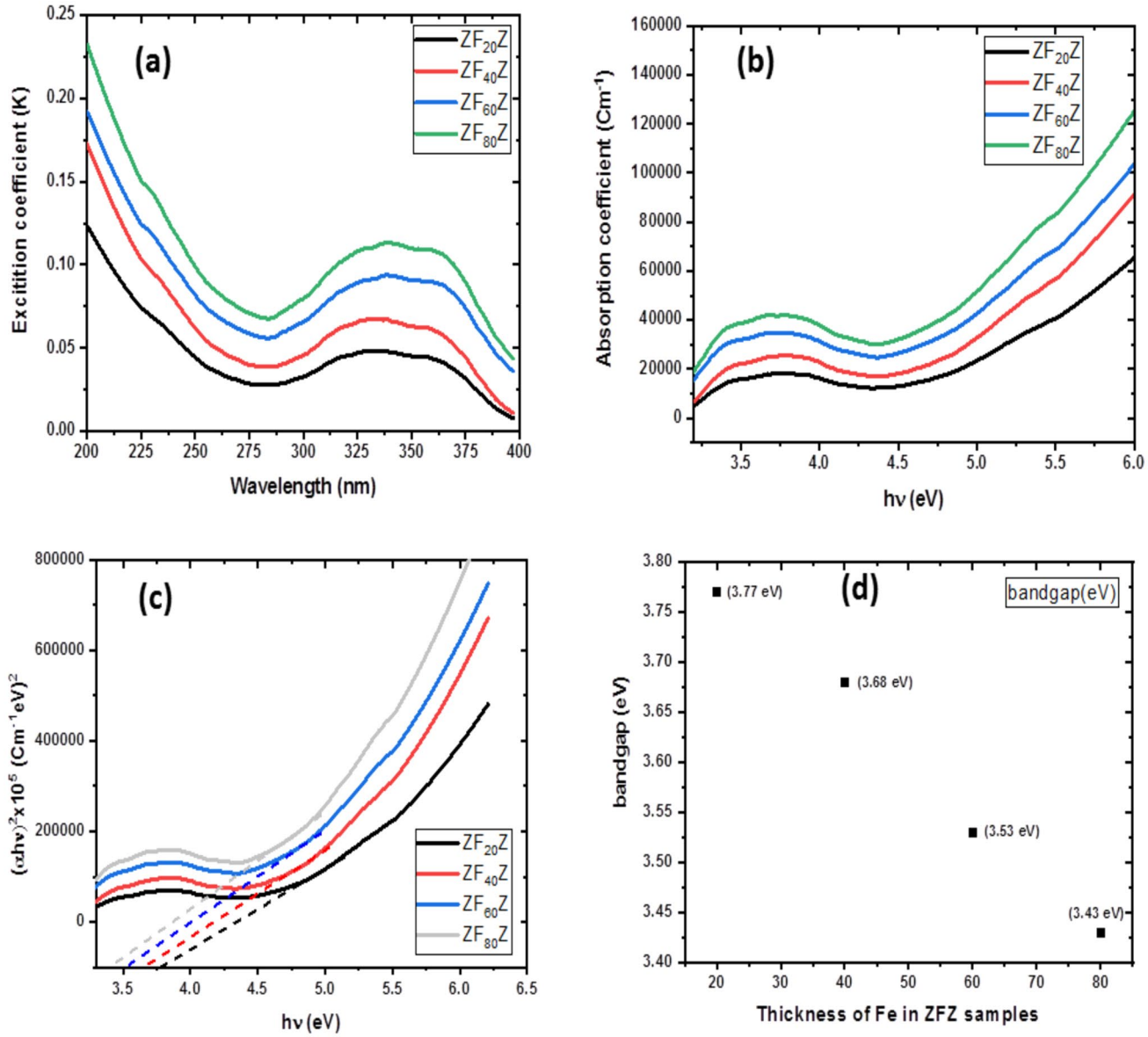

Fig. 5 Fitted values of K, α, $(\alpha h\upsilon)^2$, and E_g for $ZF_{20}Z$, $ZF_{40}Z$, $ZF_{60}Z$ and $ZF_{80}Z$ thin films

$$n = \frac{3.3668}{(Eg)^{0.32234}} \tag{6}$$

$$\frac{n^2 - 1}{n^2 + 2} = 1 - \sqrt{\frac{E_g}{20}} \tag{7}$$

The average values of the refractive index (n_{av}) estimated from the four previously mentioned equations (Eqs. 4, 5, 6, 7) are also listed in Table 1. As can be seen, the values of the n_{av} shows an increase dependence on the Fe interlayer thickness in the ZnO/Fe/ZnO system. The refractive index obtained by the four models is plotted as a function of Fe interlayer thickness in Fig. 7. Research indicates that increasing Fe concentration in ZnO/Fe/ZnO thin films can lead to changes in n, potentially, due to modifications in the films' electronic structure and density of states, depending on the Fe concentration and film properties. The refractive index is seen to increase with respect to a clear reduction in the optical energy gap which shows the inverse relationship between the refractive index and the optical energy gap. The possible explanation of the inverse relationship exists between n and E_g,

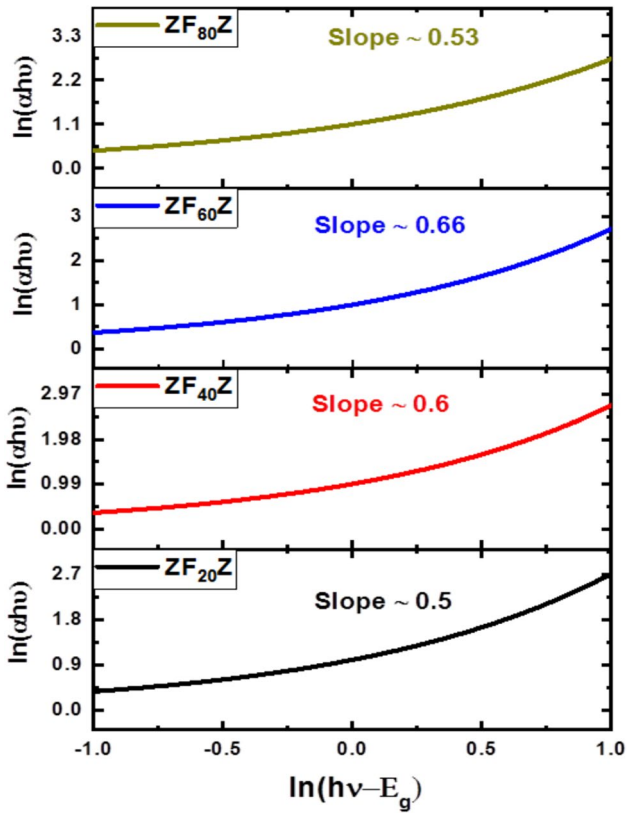

Fig. 6 Graphical presentation for determining the transition power factor for $ZF_{20}Z$, $ZF_{40}Z$, $ZF_{60}Z$ and $ZF_{80}Z$ thin films

that thin films with smaller optical energy gaps tend to have higher polarizability, leading to increase the refractive indices,and also the decrease in E_g can lead to increase in the electronic transition resulting to in higher n. Thus, it is believed that the Fe interlayer thickness plays a significant role in determining the optical energy gap and the refractive index as well.

$$\sigma_{opt} = \frac{\alpha n_{av} c}{4\pi} \tag{8}$$

The optical conductivity (σ_{opt}) is the parameter that can be used to study the electronic states of any material. The optical conductivity directly depends on the absorption coefficient and the refractive index and is found to follow the same trend as that of the absorption coefficient and the refractive index. The optical conductivity can be determined by using the following relation [27]. Where α is the absorption coefficient and c is the velocity of light.

Figure 8 Shows that optical conductivity increases with the increase in photon energy and the increase of the Fe interlayer thickness. It should be mentioned that the optical band gap in our case decreases due to which the density of number of states increases "according to density of states model" and hence the optical conductivity increase. Thus, we can be certain that the multilayer of the ZnO/Fe/ZnO thin film system shows a good photo-response, owing to their good results of optical conductivity.

3.4 The extracted parameters from the relationship of n & E_g

The relationship between the optical dielectric constant ε_{opt} and the $n_{av,}$ and the dielectric constant ε, were reported by using the relations given by [28].

$$\varepsilon = n^2 \tag{9}$$

$$\varepsilon_{(Opt)} = n^2 - 1 = \varepsilon - 1 \tag{10}$$

As observed in Table 2, and Fig. 9 the optical dielectric constant increases from 3.840 to 4.152 respectively with the increase in the concentration of Fe from 20 to 80 nm.

The dielectric susceptibility (χ_e) is a dimensionless unit, that indicates how easily any material can become transiently or completely polarized to an electric field, which in terms determines the electrical permittivity of the material. The electrical susceptibility of the four samples of the ZnO/Fe/ZnO system was calculated from the dielectric constant using the relation given [29].

Table 1 The calculated values of transition power factor (r), energy gap (E_g) and average refractive index (n_{av}) for $ZF_{20}Z$, $ZF_{40}Z$,$ZF_{60}Z$, $ZF_{80}Z$

Samples	r	(eV)	n_1 Eq. (4)	n_2 Eq. (5)	n_3 Eq. (6)	n_4 Eq. (7)	n_{av}
$ZF_{20}Z$	~0.50	3.77	2.24	2.19	2.19	2.21	2.20
$ZF_{40}Z$	~0.48	3.68	2.25	2.21	2.21	2.23	2.22
$ZF_{60}Z$	~0.52	3.53	2.27	2.24	2.24	2.26	2.25
$ZF_{80}Z$	~0.50	3.43	2.29	2.26	2.26	2.28	2.27

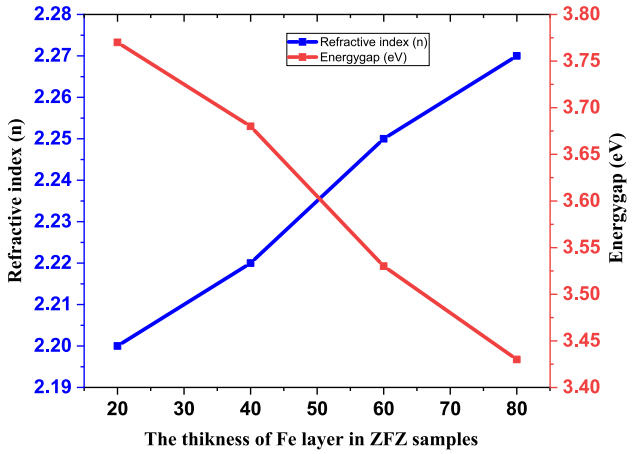

Fig. 7 Variation of refractive index with optical energy gap at different Fe interlayer thickness in the ZnO/Fe/ZnO thin film system

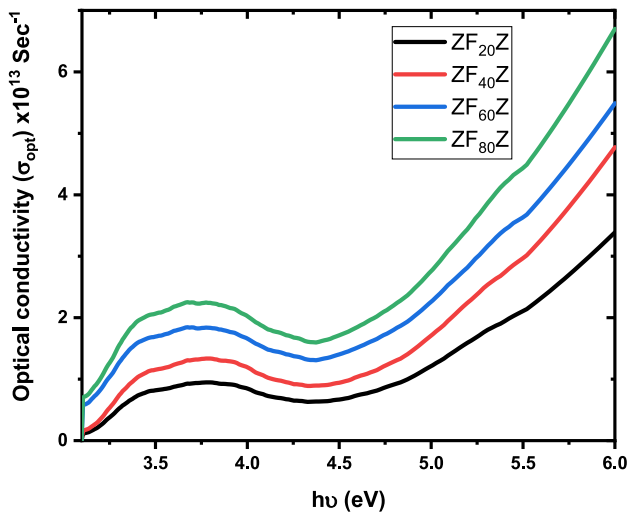

Fig. 8 Variation of the optical conductivity with photon energy for $ZF_{20}Z$, $ZF_{40}Z$, $ZF_{60}Z$ and $ZF_{80}Z$ thin films

Table 2 The calculated values of dielectric constant (ε), Optical dielectric constant (ε_{Opt}), dielectric susceptibility (χ_e) and electronic polarizability (α_e) for $ZF_{20}Z$, $ZF_{40}Z$,$ZF_{60}Z$, $ZF_{80}Z$

Samples	ε	$\varepsilon_{(Opt)}$	χ_e	$\alpha_e \times 10^{-25}$
$ZF_{20}Z$	4.840	3.840	0.305	2.226
$ZF_{40}Z$	4.928	3.928	0.312	2.248
$ZF_{60}Z$	5.062	4.062	0.323	2.280
$ZF_{80}Z$	5.152	4.152	0.330	2.301

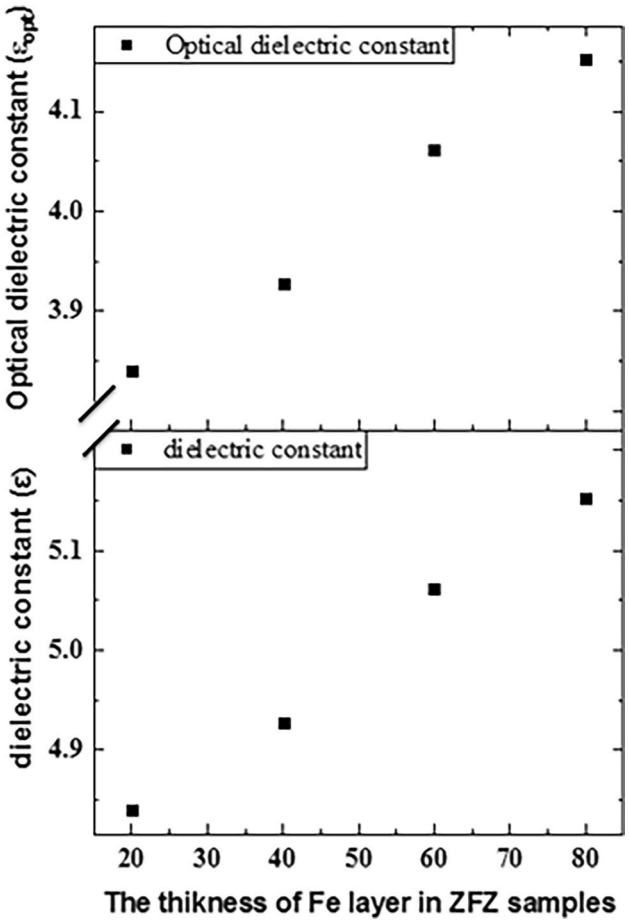

Fig. 9 Variation of the dielectric constant and optical dielectric constant with the thickness of Fe layer for $ZF_{20}Z$, $ZF_{40}Z$, $ZF_{60}Z$ and $ZF_{80}Z$ thin films

$$\chi_e = \frac{\varepsilon - 1}{4\pi} \tag{11}$$

As observed, an increase in χ_e with the increase of Fe interlayer thickness is seen in Table 2. The electronic polarizability refers to the tendency of material when subjected to an electric field, it also shows how atoms or dipoles interact with an electric field. The electronic polarizability α_e can be related to the refractive index by the following expression [30].

$$\propto_e = \frac{3(n^2-1)}{4\pi N_A(n^2+2)} \tag{12}$$

The values of α_e for the four thin films under investigation are tabulated in Table 2, while Fig. 10 presents the variation of the electrical susceptibility with the electronic polarizability.

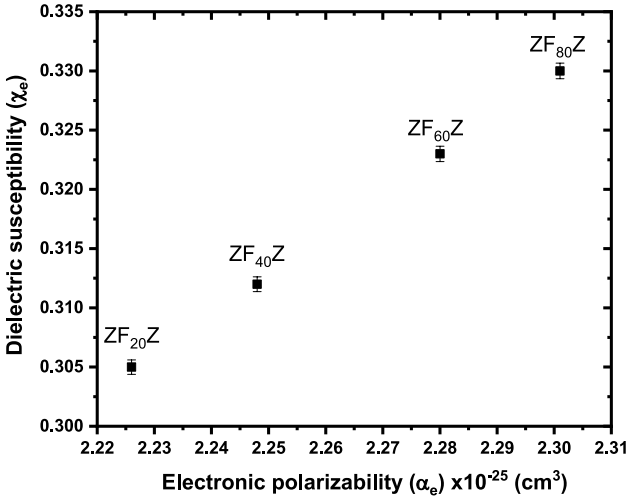

Fig. 10 Variation of the electrical susceptibility with the electronic polarizability for different Fe interlayer thickness

Table 3 Average electronegativity ($\Delta\chi$), optical basicity (Λ^0), metallization criterion (M) for ZnO/Fe/ZnO thin film system with different Fe thickness

Samples	$\Delta\chi$	Λ^0	$\frac{R_m}{V_m}$	M
$ZF_{20}Z$	1.013	1.360	0.561	0.439
$ZF_{40}Z$	0.989	1.365	0.566	0.434
$ZF_{60}Z$	0.948	1.374	0.575	0.425
$ZF_{80}Z$	0.921	1.381	0.580	0.420

It should be noted that the increase of the polarizability with the increase of Fe interlayer thickness confirm the inverse relationship between n & E_g as mentioned earlier.

As seen both the electronic polarizability and the dielectric susceptibility increase with the increase of the Fe interlayer thickness from 20 to 80nm, whereas the electrical susceptibility is related to the polarizability of the electric field by the proposed relation $\alpha_e = \chi_e E$. The correlation between the optical energy gap and the average oxide electronegativity ($\Delta\chi$), has been obtained by Duffy [31] and is given as:

$$\Delta\chi = 0.2688E_g \tag{13}$$

As observed in Table 3, the obtained $\Delta\chi$ was found to decrease with the increase of Fe thickness of $ZFe_{20}Z$, $ZF_{40}Z$, $ZF_{60}Z$ and $ZF_{80}Z$, thin films. The oxide optical basicity is related to oxide optical electronegativity and can be formulated as [32].

$$\Lambda = 1.59 - 0.2279\Delta\chi \tag{14}$$

Table 3 presented the calculated values of the optical basicity of the four samples of the ZnO/Fe/ZnO thin film samples. The value increased from 1.36 to 1.38 with the increase of Fe interlayer thickness. Molar refraction R_m is a measure of total polarization of a material. The R_m can be calculated from the molar volume V_m, and the refractive index n, *using* the Lorentz-Lorenz formula [33].

$$R_m = \left(\frac{n^2-1}{n^2+2}\right)V_m \tag{15}$$

The determined results of R_m/V_m are listed in Table 3. The metallization criterion is very important parameter for determining the tendency of the non-metallic nature of any material on the basis of its optical energy gap, and hence the refractive index as well. Herzfeld [34] has proposed a theory on metallization criterion, that explained that the refractive index become infinite for the condition $R_m/V_m = 1$, consequently for $R_m/V_m \geq 1$ the system of the materials are predicted to be metallic in in nature while in case $R_m/V_m \leq 1$ the predicted materials are non-metallic nature,or non-metallic conductors that can conduct electricity but are not metals. Understanding the relationship between metallization criteria and metal oxide is crucial for designing and optimizing devices. By exploring and controlling the link between metallization criteria and metal oxide we can develop new materials and devices, with unique performance and we can also enable tailored properties in metal oxide such as tunable conductivity or optical properties. The metallization criterion can be defined:

$$M = 1 - \left(R_m/V_m\right) \tag{16}$$

Metallization criterion on the basis of refractive index showed a decreasing trend for the four thin film samples under investigation seen in Table 3. Implies the tendency of metallization of the thin film samples of ZnO/Fe/ZnO system. The positive values of the metallization criterion suggest that the four thin films of the ZnO/Fe/ZnO thin film system are non-metallic and have relatively large refractive index. The computed values of M recorded in Table 3 shows that the present multilayer thin films behavior moves to nonmetallic nature with increasing the Fe interlayer thickness, whereas the non-metallic character refers to the tendency of an element to accept electrons to form

negative ions (anions). The $ZF_{20}Z$, $ZF_{40}Z$, $ZF_{60}Z$ and $ZF8_{80}Z$, thin films offer advantages over traditional metal conductor, and they play an important part of modern electronics and electrical engineering. Furthermore, the above property makes them ideal for use in electronic devices where low electrical resistance is required. It is important to point out that conductivity and resistivity are inversely proportional, which is clearly seen when comparing the behavior of the optical conductivity and the demined metallization for the four thin film samples under investigation. The decrease in the value of *M* from (0.339–0.420) depicts a larger width in the valence band and conduction band, which causes a decrease in the optical energy band gap from (3.77–3.43 eV).

4 Conclusions

The present work shows the various energy gap-refractive index relations and their applications behavior of a series thin film having a multilayer of ZnO/Fe/ZnO with different thickness of the Fe interlayer. The thin film under study was deposited on glass substrate by atomic layer deposition and DC magnetron sputtering techniques. The results of the X-Ray diffraction show that the reflection became more intense with the increase of Fe layer thickness,while the cross sectional images for the four samples under study proved the excellent agreement of the determined thickness with what we wanted to produce. Among the most important factors the correlation between the energy gap and the refractive index and their applications has been investigated in the above study. The physical parameters like optical conductivity, electrical susceptibility, electronic polarizability, average oxide electronegativity, oxide optical basicity and metallization criterion have been calculated based on the refractive index and energy band gap. The increase in the value of the optical and static dielectric constants indicates an increase in the optical absorption and extinction coefficient with the increase of the Fe interlayer thickness as seen in Fig. 5a,b and Table 2.The decreasing trend on the metallization criterion on the basis of the refractive index implies that the tendency of metallization is increasing with the increase of Fe interlayer thickness. The increase in the optical basicity with the increase of Fe interlayer thickness suggests that the ability of our thin film samples to donate electrons to surrounding increases. From all the above discussion the increase of Fe interlayer thickness makes our ZnO/Fe/ZnO thin film system a good basis for the prediction new non-linear optical materials.

Acknowledgements

This work was prepared at the University of Debrecen, Hungary, according to the agreement between the Faculty of Education, Ain Shams University "Coordinator and Supervisor *Prof. Dr. Suzan S. Fouad* and the Faculty of Science and Technology, the University of Debrecen" Coordinator and Supervisor *Prof. Dr. Zoltán Erdélyi*. The optical parameters were measured at the central lab of the physics department at the Faculty of Education at Ain Shams University. Project no. TKP2021- NK TA-34 has been implemented with the support provided by the National Research, development, and Innovation Fund of Hungary, financed under the TKP2021-NKTA funding scheme. Supported by the University of Debrecen Program for Scientific publication.

Author contributions

M. Nabil: Prepared all the figures, calculated the different parameters in the final form and responsible on the correspondence. S.S. Fouad: The idea and the writing and the revision. Eszter Baradács, G.Katonac, Zoltán Erdélyi: Prepared and supervising all the characteristics that had been made in Debrecen. Research.

Funding

Open access funding provided by The Science, Technology & Innovation Funding Authority (STDF) in cooperation with The Egyptian Knowledge Bank (EKB). The authors have not disclosed any funding.

Data availability

All data generated or analyzed during this study are included in this published article.

Declarations

Competing interest The authors declare that they have no conflict of interest.

Ethical approval Not Applicable.

References

1. S.S. Fouad, E. Barádacs, M. Nabil, A. Sharma, N. Mehta, Z. Erdélyi, Linearization and characterization of the Wemple–DiDomenico model of ZnO/Ni/ZnO tri-layer thin films prepared by ALD and DC magnetron sputtering. J. Alloy. Compd. **990**, 174348 (2024)
2. M. Sajjad, M.I. Inam Ullah, J.K. Khan, M. Yaqoob Khan, M.T. Qureshi, Structural and optical properties of pure and copper doped zinc oxide nanoparticles. Results Phys. **9**, 1301–1309 (2018)
3. F. Lekoui, S. Hassani, E. Garoudja, R. Amrani, W. Filali, O. Sifi, S. Oussalah, Elaboration and characterization of pure ZnO, Ag: ZnO and Ag-Fe: ZnO thin films: effect of Ag and Ag-Fe doping on ZnO physical properties. Revista Mexicana de Física (2023). https://doi.org/10.31349/revmexfis.69.051005
4. S. Sriram, A. Thayumanavan, Optical and electrical properties of nitrogen doped ZnO thin films prepared by low cost spray pyrolysis technique. J. Electron. Dev. **15**, 1215–1224 (2012)
5. V. Srikant, D.R. Clarke, On the optical band gap of zinc oxide. J. Appl. Phys. **83**(10), 5447–5451 (1998)
6. S.S. Fouad, M. Nabil, B. Parditka, A.M. Ismail, E. Baradács, H.E. Atyia, Z. Erdélyi, Assessing, surface morphology, optical, and electrical performance of ZnO thin film using ALD technique. J. Nanopart. Res. **25**(8), 172 (2023)
7. H. Zaka, B. Parditka, H.E. Zoltán Erdélyi, P.S. Atyia, S.S. Fouad, Investigation of dispersion parameters, dielectric properties and opto–electrical parameters of ZnO thin film grown by ALD. Optik **203**, 163933 (2020)
8. G.H. Kim, H.S. Kang, D.L. Kim, H.W. Chang, B.D. Ahn, S.Y. Lee, Effect of Cu dopant on the electrical property of ZnO thin films deposited by pulsed laser deposition. Solid State Phenom. **124**, 339–342 (2007)
9. S.S. Fouad, B. Parditka, M. Nabil, E. Baradács, S. Negm, H.E. Atyia, Z. Erdélyi, Bilayer number driven changes in polarizability and optical property in ZnO/TiO_2 nanocomposite films prepared by ALD. Optik **233**, 166617 (2021)
10. S.S. Fouad, B. Parditka, A.E. Bekheet, H.E. Atyia, Z. Erdélyi, ALD of TiO_2/ZnO mutilayers towards the understanding of optical properties and polarizability. Opt. Laser Technol. **140**, 107035 (2021)
11. T. Srinivasulu, K. Saritha, K.R. Reddy, Synthesis and characterization of Fe-doped ZnO thin films deposited by chemical spray pyrolysis. Modern Electron. Mater. **3**(2), 76–85 (2017)
12. Y.P. Santos, E. Valença, R. Machado, M.A. Macêdo, A novel structure ZnO-Fe-ZnO thin film memristor. Mater. Sci. Semicond. Process. **86**, 43–48 (2018)
13. T. Srinivasulu, K. Saritha, K.T. Ramakrishna Reddy, Synthesis and characterization of Fe-doped ZnO thin films deposited by chemical spray pyrolysis. Modern Electron. Mater. **3**(2), 76–85 (2017)
14. H. Bensouyad, D. Adnane, H. Dehdouh, B. Toubal, M. Brahimi, H. Sedrati, R. Bensaha, Correlation between structural and optical properties of TiO_2: ZnO thin films prepared by sol–gel method. J. Sol-Gel Sci. Technol. **59**, 546–552 (2011)
15. T. Srinivasulu, K. Saritha, K.T. Ramakrishna Reddy, Synthesis and characterization of Fe-doped ZnO thin films deposited by chemical spray pyrolysis. Modern Electron. Mater. **3**(2), 76–85 (2017)
16. H.H. Radamson, Y. Miao, Z. Zhou, Z. Wu, Z. Kong, J. Gao, G. Wang, CMOS scaling for the 5 nm node and beyond: Device, process and technology. Nanomaterials **14**(10), 837 (2024)
17. H.H. Radamson, X-ray techniques, in *Analytical methods and instruments for micro-and nanomaterials*. (Springer, Cham, 2023), pp.3–53
18. S.S. Fouad, E. Baradács, M. Nabil, G. Katona, G. Vecsei, Z. Erdélyi, Investigation of Fe thickness effect on the

absorption behavior of ZnO/Fe/ZnO tri-layers thin films. Opt. Mater. **157**, 116403 (2024)
19. A.M. Ibrahim, Some physical properties of vacuum deposited $Cd_{0.5}$ $Zn_{0.5}$ Te ternary solid solution. Vacuum **49**(1), 5–8 (1998)
20. E.A.A. El-Shazly, I.T. Zedan, K.F. Abd El-Rahman, Determination and analysis of optical constants for thermally evaporated PbSe thin films. Vacuum **86**(3), 318–323 (2011)
21. J. Yang, H. Hu, Y. Miao, L. Dong, B. Wang, W. Wang, H. Zhang, High-quality GeSn layer with Sn composition up to 7% grown by low-temperature magnetron sputtering for optoelectronic application. Materials **12**(17), 2662 (2019)
22. A.A. Al-Ghamdi, W.E. Mahmoud, S.J. Yaghmour, F.M. Al-Marzouki, Structure and optical properties of nanocrystalline NiO thin film synthesized by sol–gel spin-coating method. J. Alloy. Compd. **486**(1–2), 9–13 (2009)
23. S.S. Fouad, G.A.M. Amin, M.S. El-Bana, Physical and optical characterizations of $Ge_{10}Se_{90-}$ xTe_x thin films in view of their spectroscopic ellipsometry data. J. Non-Cryst. Solids **481**, 314–320 (2018)
24. M. Nabil, F. Horia, S.S. Fouad, S. Negm, Impact of Au nanoparticles on the thermophysical parameters of Fe_3O_4 nanoparticles for seawater desalination. Opt. Mater. **128**, 112456 (2022)
25. S.S. Fouad, M. Bence Parditka, E.B. Nabil, S. Negm, Z. Erdelyi, Effect of Cu interlayer on opto-electrical parameters of ZnO thin films. J. Mater. Sci. Mater. Electron. **33**, 20594–20603 (2022)
26. S.S. Fouad, E. Baradacs, M. Nabil, B. Parditka, S. Negm, Z. Erdelyi, Microstructural and optical duality of TiO_2/Cu/TiO_2 trilayer films grown by atomic layer deposition and DC magnetron sputtering. Inorg. Chem. Commun. **145**, 110017 (2022)
27. Z.K. Heiba, M.B. Mohamed, A. Badawi, Effect of vanadium doping on the structural and optical characteristics of Nano ZnCdS. Phys. Scr. **97**(5), 055802 (2022)
28. S.A. Umar, M.K. Halimah, K.T. Chan, A.A. Latif, Polarizability, optical basicity and electric susceptibility of Er3+ doped silicate borotellurite glasses. J. Non-Cryst. Solids **471**, 101–109 (2017)
29. M.S. Dresselhaus, M.S. Dresselhaus, J. Tauc, Optical properties of solids. Part II, book (1998)
30. V. Dimitrov, T. Komatsu, An interpretation of optical properties of oxides and oxide glasses in terms of the electronic ion polarizability and average single bond strength. J. Univ. Chem. Technol. Metall **45**(3), 219–250 (2010)
31. J.A. Duffy, Electronic polarizability and related properties of the oxide ion. Phys. Chem. Glasses **30**, 1 (1989)
32. D.B. Thombre, The Estimation of oxide polarizability and basicity using electronegativity for B_2O_3: M_2O glass system (M = Li, Na, K, Rb). Int. J. Innov. Sci. Eng. Technol. **3**, 449–453 (2016)
33. B. Bhatia, S.L. Meena, V. Parihar, M. Poonia, Optical basicity and polarizability of Nd3+-doped bismuth borate glasses. New J. Glass Ceram. **5**(3), 44–52 (2015)
34. K.F. Herzfeld, On atomic properties which make an element a metal. Phys. Rev. **29**(5), 701 (1927)